

# Differential Hanle effect and the spatial variation of turbulent magnetic fields on the Sun

J.O. Stenflo<sup>1</sup>, C.U. Keller<sup>2</sup>, and A. Gandorfer<sup>1</sup>

<sup>1</sup> Institute of Astronomy, ETH Zentrum, CH-8092 Zürich, Switzerland

<sup>2</sup> National Solar Observatory, P.O. Box 26732, Tucson, AZ 85726-6732, USA

Received 9 May 1997 / Accepted 3 September 1997

**Abstract.** While diagnostic techniques based on the ordinary Zeeman effect (e.g. magnetograms) are almost “blind” to a turbulent magnetic field with mixed magnetic polarities within the spatial resolution element, the Hanle effect is sensitive to this domain of solar magnetism. We present observational evidence that the turbulent magnetic field that fills the 99% of the volume between the kG flux tubes in quiet solar regions does not have a unique field-strength distribution, but the rms turbulent field strength can vary by an order of magnitude from one solar location to the next.

The varying Hanle depolarization in combinations of spectral lines with different sensitivities to the Hanle effect is conspicuously evident from direct visual inspection of the spectra. To quantify these variations we have extracted the polarization amplitudes for a selection of spectral lines observed in 8 different solar regions with different turbulent field strengths, and then applied an inversion technique to find the field strengths and calibrate the selected lines. The inversion gives stable solutions for the turbulent field strengths, in the range 4–40 G, but the field-strength scale is presently very uncertain.

The inversion exercise has helped to expose a number of problem areas which need to be attended to before the differential Hanle effect can become a standard, reliable diagnostic tool. One major problem is the extraction of the line polarization when the contributions from the line and continuum are of the same order of magnitude, which is the usual case. For exploratory purposes we have applied a heuristic, statistical approach to deal with this problem here.

**Key words:** polarization – scattering – Sun: magnetic fields – atomic processes – radiative transfer

---

## 1. Introduction

The linearly polarized solar spectrum that is produced by coherent scattering has a structural richness that is comparable to that of the intensity spectrum, but its appearance is entirely

different, and the spectral structures are due to different physical processes (Stenflo & Keller 1996, 1997; Stenflo 1997). This spectrum, which has been referred to as the “second solar spectrum”, provides us with a new window for diagnostics of the Sun. In the present paper we will explore the potential use of the second solar spectrum as a tool to diagnose magnetoturbulence on the Sun.

The physical process that provides novel and unique diagnostic possibilities is the *Hanle effect*, which can only be accessed through the second solar spectrum, since it is fundamentally a coherence phenomenon that can only occur when there is coherent scattering. Due to its richness in spectral features the second solar spectrum allows multiple-line diagnostics with combinations of many different spectral lines that have different sensitivities to the Hanle effect. This type of approach has proven extremely useful in the past for Zeeman-effect diagnostics to derive information on the “hidden” magnetic fine structure that exists on small scales beyond the spatial resolution limit (Stenflo 1973, 1994; Solanki 1993). With a *differential* approach much of the previous model dependence in the observations can be avoided, and one may develop semi-empirical models of the magnetic structures that are far more sophisticated and realistic than would otherwise be possible.

Diagnostic techniques based on the ordinary Zeeman effect however have a fundamental limitation: As the sign of the signal depends on the orientation of the magnetic field, the contributions from opposite polarities within the spatial resolution element cancel each other, such that to first order only the uncanceled portion gives a net signal that is available to Zeeman-effect diagnostics. There are two exceptions to this statement: (i) If the directional distribution of the field vectors is not isotropic, then there is not complete cancellation of the linear polarization due to the transverse Zeeman effect, and this can be used to constrain the distribution (Stenflo 1987). (ii) If the field-strength distributions for the two magnetic polarities are not identical, then the circular polarization of the longitudinal Zeeman effect can provide information on the subresolution fields if the Zeeman splitting is large enough, even when the opposite-polarity fluxes are perfectly balanced (Rüedi et al. 1992; Solanki 1993).

---

Send offprint requests to: J.O. Stenflo

This limitation does not apply to the Hanle effect, which for mixed-polarity fields reduces the amount of scattering polarization from its maximum value in the absence of magnetic fields. The depolarization works with one sign, i.e., in one direction, regardless of the field polarity. This unique property was first used to constrain the strength of a volume-filling, turbulent photospheric magnetic field to be somewhere in the range 10–100 G (Stenflo 1982). With detailed numerical modelling of the polarized radiative transfer in the Sr I 4607 Å line Faurobert-Scholl (1993) and Faurobert-Scholl et al. (1995) could develop this approach into a more definite quantitative diagnostic tool and found that the turbulent field must be 10–30 G to fit the Sr I observations of Stenflo et al. (1980). Other areas where the Hanle effect has established its usefulness are diagnostics of solar prominences (Leroy et al. 1977; Sahal-Bréchet et al. 1977; Bommier 1980; Landi Degl’Innocenti 1982; Querfeld et al. 1985) and chromospheric magnetic canopies (Faurobert-Scholl 1992, 1994).

Interpretations that are based on observations of a single spectral line are however sensitive to the model used for the solar atmosphere and the atomic physics. As in Zeeman-effect diagnostics one can suppress such model dependence by using the *differential* rather than the absolute polarization effects, which are seen in combinations of lines with different sensitivities to the Hanle effect.

Our previous concept of solar magnetism (outside active regions) has been basically that of a 2-component atmosphere. Zeeman-effect diagnostics have shown that the major part of the net solar magnetic flux that is seen with a spatial resolution corresponding to a smearing window of one arcsec or larger originates in concentrated, intermittent kG “flux tubes”, which occupy a tiny fraction of the photospheric volume, less than one percent in quiet solar regions. The remaining 99 % that appear more or less non-magnetic to Zeeman-effect diagnostics must (unless it is truly field free, which is hardly possible in the real physical world) contain some sort of tangled or turbulent magnetic field, since Zeeman-effect observations are almost “blind” to such a field if the magnetic polarities are mixed on a sub-resolution scale. If the mixing is only partial, or if the polarities are spatially partly resolved, e.g. in the case of the intranetwork fields, then Zeeman-effect diagnostics will of course still be useful.

The Hanle effect on the other hand is practically blind to the flux tube field, since this field has such a small filling factor, and the Hanle effect is insensitive to vertical magnetic fields when the illumination of the scattering particles is axially symmetric. Almost the entire contribution to the Hanle effect comes from the 99 % of the volume to which the ordinary Zeeman effect is almost blind. The Hanle and Zeeman effects therefore ideally complement each other.

Since the flux tube field strength has been found to have an almost unique value of about 1.5 kG in quiet network regions at the level in the solar atmosphere where the continuum around 5000 Å from the surrounding atmosphere is formed, it has been natural to believe that the turbulent, space-filling magnetic field should also have a unique field distribution with an rms field

strength that is uniquely determined by the kinetic energy spectrum of the solar granulation. Accordingly it has been expected that the turbulent rms field strength should be nearly invariant with respect to time and location and therefore be a unique quantity that needs to be determined once and for all.

This view of solar magnetism was shaken when we in February 1996 started to record the same portions of the second solar spectrum in different regions on the Sun (at the same limb distance but at different position angles). We found to our surprise that the appearance of the spectral variations of the scattering polarization could change drastically from one spatial location to the next. While being able to rule out instrumental effects (including instrumental polarization), we know of no other solar causes than spatial variations of the magnetic-field effects across the solar disk. The discovery of these spatial variations appears to imply that the properties of the turbulent or tangled magnetic field are not invariant but that the turbulent field strength is a quantity that needs to be mapped.

In the present paper we present examples of these spatial variations and make an attempt to use the observed differential effects for combinations of lines in the second solar spectrum to explore the new diagnostic possibilities and to uncover problem areas. Our so far heuristic approach leads to quantitative estimates of the turbulent field strengths based on the differential Hanle effect without having to enter into radiative transfer calculations. We find that the turbulent field strength can easily vary by an order of magnitude. However, we cannot rule out that varying canopy-like fields also affect the interpretations.

## 2. General conditions for the solvability of the Hanle diagnostic problem

The Hanle depolarization due to a magnetic field can be expressed in terms of the factor  $k_H^{(2)}$ , which represents the ratio between the observed polarization amplitude  $p_{\text{line}}$  in the selected spectral line and the corresponding amplitude  $p_0$  in the absence of a magnetic field. Thus

$$p_{\text{line}} = k_H^{(2)} p_0. \quad (1)$$

The (2) in the upper index position of  $k_H$  refers to the  $2K$ -multipole and the circumstance that it is the multipole with  $K = 2$  (the electric quadrupole) that is responsible for atomic alignment and the linear polarization (while  $K = 1$  (magnetic dipole, atomic orientation) governs the scattering of the circular polarization).

For the fields that we will be dealing with here the Zeeman splitting is much smaller than the Doppler width. In this case the Hanle depolarization factor  $k_H^{(2)}$  for a turbulent magnetic field of strength  $B_t$  with an isotropic distribution of field vectors is according to Stenflo (1982) given by

$$k_H^{(2)} = 1 - 0.4 \left( \frac{1}{1 + 4/\Omega^2} + \frac{1}{1 + 1/\Omega^2} \right), \quad (2)$$

where

$$\Omega = \frac{2B_t}{B_0/k_c^{(2)}}. \quad (3)$$

Here we have introduced two new quantities, the “characteristic field strength”  $B_0$  for which the Hanle effect is sensitive, and the collisional branching ratio  $k_c^{(2)}$  for the  $2K$ -multipole (with  $K = 2$ ). In SI units

$$B_0 = \frac{2m\gamma_N}{eg_e}, \quad (4)$$

where  $m$  and  $e$  are the mass and charge of the electron,  $g_e$  is the Landé factor of the excited level, and  $\gamma_N$  is the natural decay rate of the excited state (due to spontaneous emission). For a field of strength  $B_0$  the Larmor precession frequency is comparable to the decay rate (or inverse life time)  $\gamma_N$ .

$$k_c^{(2)} = \frac{\gamma_N}{\gamma_N + 0.5\gamma_c}, \quad (5)$$

where  $\gamma_c$  is the collisional broadening rate, and  $0.5\gamma_c$  represents the rate at which the  $2K$ -multipole is collisionally destroyed (Stenflo 1994; Faurobert-Scholl et al. 1995).  $B_0/k_c^{(2)}$  thus represents the effective characteristic field strength of the Hanle effect that results when we compare the Larmor frequency with the total destruction rate of the atomic polarization of the excited state due to the combined effect of spontaneous decay and collisions.

If we could somehow determine the Hanle depolarization factor  $k_H^{(2)}$  from observational data, we could find  $\Omega$  from Eq. (2) and  $B_t$  from Eq. (3), provided that the effective characteristic field strength  $B_0/k_c^{(2)}$  is known. Assuming that we can determine the line polarization  $p_{\text{line}}$  from the observations (which turns out to be a complex task due to the continuum polarization, see below),  $k_H^{(2)}$  still cannot be found directly from Eq. (1), since the amplitude  $p_0$  in the absence of magnetic fields is in general an unknown quantity. Furthermore, while the field strength parameter  $B_0$  can sometimes be found from atomic physics data (if the natural life time and Landé factor of the excited state are known), the collisional branching ratio  $k_c^{(2)}$  depends both on the atmospheric densities and temperatures and on the atomic physics. This general problem was solved by Faurobert-Scholl (1993) and Faurobert-Scholl et al. (1995) by doing sophisticated radiative-transfer modelling to calculate  $p_0$  and  $k_c^{(2)}$  for the Sr I 4607 Å line.

If we want to avoid such radiative-transfer modelling, then we are stuck with three unknowns,  $B_0/k_c^{(2)}$ ,  $p_0$ , and  $B_t$ , while there is only one observable,  $p_{\text{line}}$  (assuming that we are able to separate the line contribution from the observed total polarization of both continuum and line). The problem may thus appear unsolvable. This is however so only if we consider a single spectral line. The number of observables and unknowns multiply at different rates when we observe several spectral lines in several different solar regions. If the numbers of lines and regions are sufficiently large, one passes a cross-over, beyond which the number of observables is larger than the number of unknowns and the problem becomes solvable. Let us now make the book-keeping to see when this cross-over takes place.

Let us assume that we have an observational data set from which we are able to extract the empirical line polarizations  $p_{\text{line}}$  for  $n_\ell$  different spectral lines in  $n_r$  different regions on the

Sun, which all have the same limb distance but different field strengths  $B_t$ . There are two unknowns ( $B_0/k_c^{(2)}$  and  $p_0$ ) and one observable ( $p_{\text{line}}$ ) per spectral line, while there is one new unknown ( $B_t$ ) for each solar region. The number of unknowns is thus  $2n_\ell + n_r$ , while the number of observables is  $n_r n_\ell$ . The necessary (although not necessarily sufficient) condition for the problem to be solvable is then

$$n_r n_\ell \geq 2n_\ell + n_r, \quad (6)$$

or

$$n_\ell \geq \frac{n_r}{n_r - 2}. \quad (7)$$

A solution is thus possible only if we can observe the  $n_\ell$  lines in at least 3 different solar regions with different turbulent field strengths  $B_t$ . If  $n_r = 3$ , then we must have  $n_\ell \geq 3$ .

The problem can be extended further by adding more free parameters, but there will always be a cross-over such that with a sufficient number of spectral lines and solar regions observed, the number of observables will exceed the number of unknowns. For instance, there is always some uncertainty in the precise limb distance of a given observation, and since the polarization amplitude varies steeply with limb distance, one could apply a scaling factor as a free parameter to all the lines that are covered within the spectral field of view. This would compensate for an error in the limb distance (assuming that all the covered lines have a center-to-limb dependence with the same relative steepness). One could also introduce an extended parametrization to model the turbulent magnetic field and let it be described not just by a single field strength, but by a parametrized distribution of field strengths. The collisional depolarization factor  $k_c^{(2)}$  could in principle also be allowed to vary from one solar region to the next.

The circumstance that one can always assemble a data set for which the number of observables exceeds the number of unknowns does however by no means guarantee that the problem can be solved, i.e., that the inversion will have a unique solution. For the inversion problem to be well conditioned it is necessary that the selected spectral lines have a large spread in their sensitivities to the Hanle effect (i.e., in their  $B_0/k_c^{(2)}$  values), and that the selected solar regions have a large spread in their  $B_t$  values (within the Hanle sensitivity range of the selected set of lines). Furthermore the empirical line polarization  $p_{\text{line}}$  must be a well defined quantity. Surprisingly enough, this last point turns out to be the biggest problem.

If there were no continuum radiation, then  $p_{\text{line}}$  in Eq. (1) would be the directly observed polarization amplitude in the line. In reality, however, the spectral lines are superposed on a background continuum that is polarized. For most lines near the solar limb (like at  $\mu = 0.1$ ) the continuum polarization is of the same order of magnitude as the line polarization, with the exception of a few particularly strongly polarizing lines, like Ca I 4227 Å, Sr I 4607 Å, and Na I D<sub>2</sub>. Unfortunately the line polarization cannot simply be measured from the continuum level, since for large Hanle depolarizations the observations show (see

below) that the polarization in the line can lie far below the continuum level. The Hanle depolarization cannot lead to a change in sign of the polarization, only to a reduction of the line polarization amplitude with a certain, magnetic-field dependent factor. All values of the observed line polarization  $p_{\text{line}}$  in Eq. (1) have to be positive to be “physical” and for the inversion procedure to work. To extract  $p_{\text{line}}$  from the observations we have to define some reference level from which the observed polarization should be measured to represent the line polarization. However, due to the mixing of the polarizing line and continuum opacities this reference level is neither the polarization zero level nor the level of the continuum polarization beside the line, but something in between.

This problem is further aggravated by the circumstance that Stokes  $I \rightarrow Q$  cross talk (due to instrumental polarization) makes the zero level of the polarization scale unknown when working with telescopes that are not polarization free (Stenflo & Keller 1997).

In spite of these difficulties we have carried out an observing project to measure a large number of spectral lines in as many solar regions as possible that have the same limb distance ( $\mu = 0.1$ ) but have clearly different Hanle depolarizations, which can be verified by direct inspection of the qualitative appearance of the polarized spectra. A heuristic way of defining a reference level for the line polarization is found after some experimentation with the data, and the inversion problem is solved after careful conditioning of the data set to avoid the condition that the problem is ill posed. The inversion finds turbulent field strengths in the range 4–40 G for the various solar regions. One main aim of this exercise is to expose the various problems that have to be addressed and solved before the Hanle effect can be considered to be a reliable and well established diagnostic tool for exploring magnetic fields on the solar disk.

### 3. Observational material and data reduction procedure

All the observations used here have been obtained with the ZIMPOL I polarimeter (cf. Povel 1995; Stenflo & Keller 1997) at a disk position of  $\mu = 0.1$  (corresponding to a limb distance of 5 arcsec). Three spectral regions that contained a particularly high concentration of polarization structures due to atomic (rather than molecular) transitions were selected: 4884–4888 Å, 4931–4936 Å, and 5682–5687 Å. In these three wavelength ranges 20 polarization features were identified as potentially useful candidates for Hanle diagnostics.

The recordings of these lines were done in 8 different solar regions (all at  $\mu = 0.1$ ) during three different observing runs with ZIMPOL I at the McMath-Pierce facility of NSO/Kitt Peak. While 6 of the regions were recorded in September 1996, one was recorded in April 1995 and one in February 1996. Most of the solar regions were selected at different position angles near the geographic north or south position of the solar limb, while one region was near the geographic east limb.

As the main objective of the present work is to explore the diagnostic potential of the differential Hanle effect and identify problem areas to be addressed by future work, rather than to

present definite quantitative results on field strength and line parameters, we refrain here from listing all the technical details concerning the observations and the selected lines.

#### 3.1. Evidence for varying turbulent magnetic fields

Fig. 1 provides examples of spectra for the 4886 and 4934 Å wavelength ranges. The top panels show the usual intensity spectra, which hardly vary from region to region on the Sun (as long as the limb distance is kept fixed), while the panels below show the “second solar spectrum” (linear polarization or  $Q/I$ ) for two solar regions that differed greatly in Hanle depolarization. The inversions that we will comment on later give turbulent field strengths  $B_t$  of 4 and 30 G, respectively, for these two regions.

Regardless of whether one trusts these quantitative values or not, it is apparent from direct visual inspection of the  $Q/I$  spectra that the polarizations in the bottom panels are subject to much more Hanle depolarization than the  $Q/I$  spectra of the middle panels. One may therefore immediately draw the qualitative conclusion, without any modelling or special assumptions, that the turbulent fields of the solar region that is represented by the bottom panels are much stronger than those of the region that is represented by the middle panels. The inversions merely try to quantify this direct conclusion in terms of G units.

The different spectral regions could not be recorded simultaneously, and in some cases the time separation could be as large as 1–2 days for the “same” solar region. Due to solar rotation the heliographic location is then not identical. However, at  $\mu = 0.1$  at high latitudes and with our crude spatial resolution (including averaging along the 50 arcsec long slit), this difference may not be so important here. This could be seen in Fig. 5 of Stenflo & Keller (1997), where recordings separated in time by two days were plotted on top of each other.

It is interesting to note that although both the solar regions that are represented in Fig. 1 were located at the position angle of geographic north, which was at almost the same distance from the heliographic north pole in both cases (about 25°, but on opposite sides of the heliographic pole), the turbulent field strength differs dramatically, by a factor of about 8 according to the inversions. This difference can be due to both spatial and temporal changes (since the observations were separated in time by 1½ years). Whatever the cause, it demonstrates that the turbulent field does not have an invariant field strength distribution, but its properties need to be mapped in space and time.

Let us here again stress that Zeeman-effect or magnetograph observations are blind to this type of field. Use of the Hanle effect is the only real avenue that we have to access this domain of magnetoturbulence.

#### 3.2. Extraction of the line polarization

As has been noted above, the zero point of the polarization scale is unknown, so we have to rely on theoretical or indirect considerations to estimate its location. Here we will use heuristic arguments in connection with the definition of a procedure to

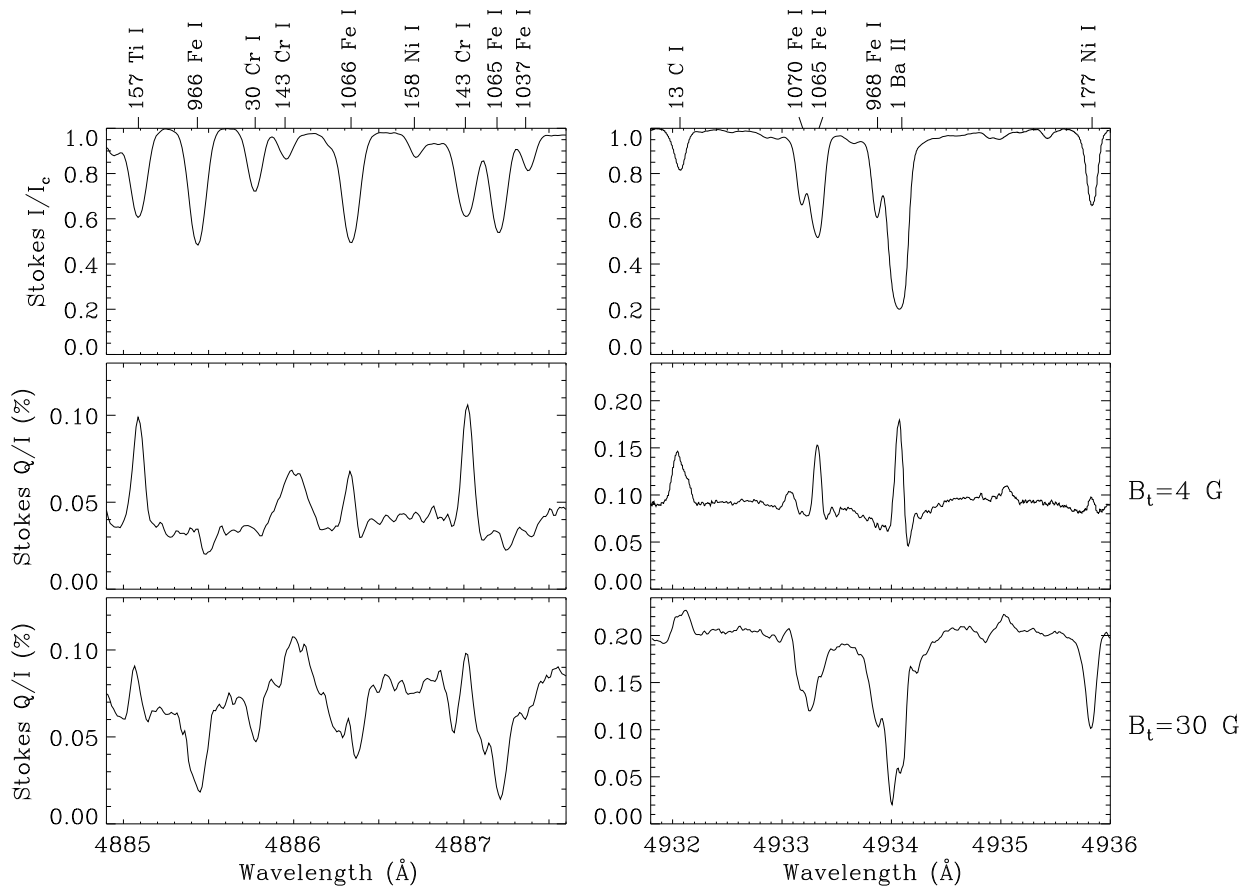


**Fig. 1.** Examples of varying Hanle depolarization on the solar disk. For each of the wavelength ranges 4885–4888 Å and 4932–4936 Å the top panel shows the intensity  $I$  (normalized to the local continuum intensity  $I_c$ ) with line identifications and multiplet numbers, while the two lower panels show the fractional linear polarization  $Q/I$  for two solar regions (which are the same for the two wavelength ranges), one with little (middle panel) and one with much (bottom panel) Hanle depolarization. No attempt has been made here to fix the zero point of the polarization scale, which is thus arbitrarily chosen, but it is unimportant for the qualitative comparison of the two solar regions. According to our inversions the turbulent field strength  $B_t$  has a value of 4 and 30 G for these two regions, which were recorded respectively on 4–5 April 1995 and 15 September 1996 with the spectrograph slit 5 arcsec inside the limb at the position angle of geographical north, using ZIMPOL I at the McMath-Pierce facility of NSO/Kitt Peak.

extract a quantity that would represent the line polarization  $p_{\text{line}}$ , as we will discuss next.

Previous surveys of the second solar spectrum (Stenflo et al 1983a,b) have indicated that there is a statistical relation between the shapes  $(p_c - p)/p_c$  of the depolarizing, absorption-like  $Q/I$  profiles of lines with apparently no intrinsic polarization, and their intensity profiles  $(I_c - I)/I_c$ . Here  $p_c$  and  $I_c$  are the polarization and intensity of the continuous spectrum. A simple and natural way to parametrize this relation in terms of one free parameter  $\alpha$  is to write

$$\frac{p_c - p_z}{p_c} = \left( \frac{I_c - I}{I_c} \right)^\alpha. \quad (8)$$

Here we have written  $p_z$  instead of  $p$  to mark that the above relation is supposed to apply to non-scattering lines with no intrinsic polarization. If a line does contribute with some intrinsic scattering polarization, then this contribution would in the framework of this heuristic model be added on top of  $p_z$ . Accordingly the

intrinsic line contribution to the observed polarization  $p$  is given by

$$p_{\text{line}} = p - p_z. \quad (9)$$

$p_z$  thus represents a kind of zero or reference level to be used for the extraction of the line contribution  $p_{\text{line}}$ .

In reality the continuum and line polarizations are entangled in a non-linear way, which can only be properly modelled with radiative transfer. Our extraction procedure here in terms of Eqs. (8) and (9) with the introduction of an “intrinsic” line polarization  $p_{\text{line}}$  is thus mainly formal, to allow us to more explicitly illustrate the diagnostic possibilities of the differential Hanle effect. In our ZIMPOL observations we do not find any purely depolarizing lines that could serve as good references. This, in combination with the unknown zero point of the polarization scale, makes the whole extraction procedure questionable and error prone, but without it we would have no quantity to which

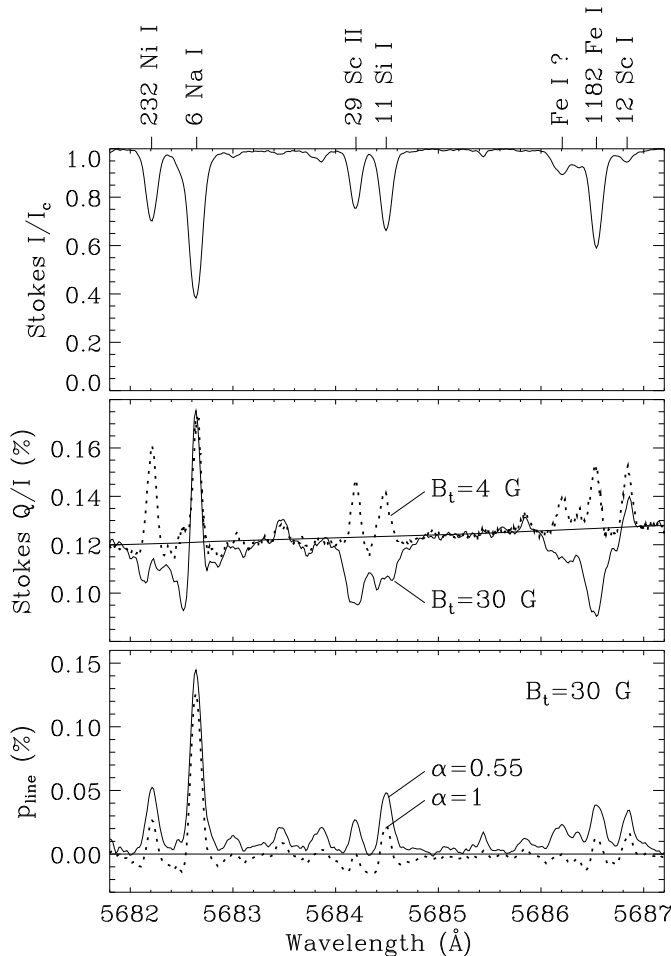


**Fig. 2.** Illustration of the differential Hanle effect and the procedure for extracting the line polarization  $p_{\text{line}}$  for the wavelength range 5682–5687 Å. Top panel: Intensity spectrum, normalized to the local continuum. Middle panel: Fractional polarization  $Q/I$  for the same two solar regions, with  $B_t = 4$  G (dotted curve) and 30 G (solid curve), which were shown in Fig. 1. The recordings were made on the same days and with the same equipment as those of Fig. 1. The continuum polarization level is slanted due to a wavelength dependence of the instrumental  $I \rightarrow Q$  cross talk. Bottom panel: Two attempts to extract the line polarization  $p_{\text{line}}$  from the  $Q/I$  spectrum in the middle panel that corresponds to 30 G. Only with a value as small as 0.55 for the profile shape parameter  $\alpha$  do all  $p_{\text{line}}$  values become positive for all lines and solar regions, but some spurious features may also be produced by this heuristic procedure.

a Hanle depolarization factor could be applied (since so far nobody has the capabilities to do proper simulations of these lines with polarized radiative transfer).

Assuming that we have defined the value of  $\alpha$  and the position of the zero point of the polarization scale (see below), then the formal extraction procedure is straightforward. From the intensity spectrum we get  $I$  and  $I_c$ , which gives us the  $p_z$  profile via Eq. (8). This is then subtracted from the observed  $p$  ( $= Q/I$ ) spectrum, which via Eq. (9) gives us  $p_{\text{line}}$ .

While previous work (Stenflo et al. 1983a,b) has suggested that  $\alpha = 1$ , implying a direct proportionality between the profile shapes, our present data indicate that a substantially smaller value of  $\alpha$  is needed. This can be seen in Fig. 2, where we have illustrated the situation for the third of our selected wavelength ranges, 5682–5687 Å. As usual the top panel shows the intensity spectrum, while the middle panel shows the observed Stokes  $Q/I$  for the same two solar regions that were chosen for Fig. 1. The 4 and 30 G regions are represented by the dotted and solid curves, respectively. A common straight line has been fitted through the continuum points to represent the level of the continuum polarization. This level is slanted, because the slow wavelength dependence of the instrumental polarization ( $I \rightarrow Q$  cross talk) makes the position of the zero point of the polarization scale vary with wavelength. The magnitude and sign of the gradient (slope) is consistent with theoretical calculations of the wavelength dependence of the instrumental polarization of the McMath-Pierce telescope and the compensating glass plate. The zero level in the diagram has been chosen to optimize the procedure for the extraction of  $p_{\text{line}}$  (see below).

The bottom panel of Fig. 2 shows two versions of  $p_{\text{line}}$ , both of which have been extracted from the solid  $Q/I$  curve with  $B_t = 30$  G in the middle panel. Thus the profile form parameter  $\alpha = 1$  for the dotted curve, 0.55 for the solid curve. The model with  $\alpha = 1$  is unable to make all the values of  $p_{\text{line}}$  positive for any reasonable choice of the polarization zero level. One can see that a substantially smaller value of  $\alpha$  is needed, since the depolarizing  $Q/I$  profiles are generally broader than the corresponding intensity profiles, and a smaller  $\alpha$  is needed to mimic this change in profile shape. Assuming that there is no subtle contribution from the transverse Zeeman effect mixed in our  $Q/I$  data, we find that an  $\alpha$  as small as about 0.55 is needed to make the values of  $p_{\text{line}}$  positive for *all* our spectral lines and *all* our solar regions.

Choosing a value for  $\alpha$  is however not the only thing that we have to do to define  $p_z$  and  $p_{\text{line}}$ , since the scale of the observed polarizations has an unknown zero point, which is common for all three quantities  $p$ ,  $p_c$ , and  $p_z$ . If we use a theoretical value for  $p_c$  in combination with the observed continuum level to determine the zero point, then we are unable to always get positive  $p_{\text{line}}$  values for *any* value of  $\alpha$ . We are forced to choose another, considerably higher value for  $p_c$  to make our heuristic concept of a  $p_{\text{line}}$  self-consistent. This in turn suggests that current theoretical modelling of the continuum polarization is inadequate, but this is a separate problem that is outside the scope of the present paper.

Another uncertainty is our assumption that the line polarization must always be a positive quantity to be “physical”. As has been shown by Faurobert-Scholl (1994), this is not always a valid assumption, since some special magnetic configurations may lead to negative polarizations in some spectral lines, in particular in chromospheric canopies. However, for turbulent fields in the photosphere negative polarizations should normally not occur.

Thus, by exploring the two-parameter  $\alpha$ – $p_c$  space, we have estimated the minimum value of  $p_c$  and the maximum value

of  $\alpha$  (0.55) that always give “physical” (positive)  $p_{\text{line}}$  values. These values of  $p_c$  and  $\alpha$  have then been used to fully define the procedure for extracting  $p_{\text{line}}$  from the data. Since the continuum data points can be fitted with a straight line, the choice of a value for  $p_c$  defines the zero point of the polarization scale.

This heuristic procedure is of course very unsatisfactory, but it is the best that we can do for the time being. Unfortunately it may also produce spurious polarization features, as suggested by Fig. 2 at places, where no obvious features are seen in  $Q/I$ , e.g. at  $\lambda 5685.4 \text{ \AA}$ . There is clearly an urgent need to explore the continuum polarization, both empirically and theoretically, to model the behavior of depolarizing lines, and to control the instrumental polarization.

#### 4. Inversions

With 20 spectral lines ( $n_\ell = 20$ ) and 8 solar regions ( $n_r = 8$ ), our inversion problem has  $2n_\ell + n_r = 48$  unknowns ( $B_0/k_c^{(2)}$  and  $p_0$  for each line, and  $B_t$  for each region). If all 20 lines were recorded in all of the 8 regions, there would be  $n_\ell n_r = 160$  observables, but since the observations did not have this degree of completeness, the actual number of “observables” ( $p_{\text{line}}$  values) was 99.

Several of the 20 lines were unidentified or blended and therefore of questionable usefulness for Hanle diagnostics. As such lines may contribute to making the inversion problem severely ill posed, it is necessary to first condition the problem by exploring the degree of consistency in the behavior of the different spectral lines, to sort out before the inversion those lines that do not exhibit any consistent pattern with respect to the Hanle effect. This sorting was done as follows.

For a given spectral line the extracted values of  $p_{\text{line}}$  should decrease with increasing value of  $B_t$  for the solar regions. If one ranks the different solar regions in terms of their  $p_{\text{line}}$  values, this ranking should be approximately the same for all the spectral lines if one ignores the difference in height of formation and the variation of  $B_t$  with height. In practice the rankings are not identical for all the lines, e.g. because of measurement errors, an invalid procedure for determining  $p_{\text{line}}$ , or different formation heights of the lines. Still there turns out to be a high degree of consistency between the different rankings, which is encouraging and indicates that our procedure is at least partially valid.

To explore the consistency behavior of the lines we first determine for each line and region the normalized line polarization  $p_{\text{norm}} = p_{\text{line}}/p_{\text{line, max}}$ , where  $p_{\text{line, max}}$  is the maximum value of  $p_{\text{line}}$  among the 8 solar regions for a given spectral line. The normalization is done to avoid giving undue weight to lines with high polarization amplitudes. Then we determine for each solar region the average of  $p_{\text{norm}}$  over all the spectral lines. This average is then used to rank the solar regions in a sequence of monotonically increasing  $B_t$  (the numerical values of which are so far entirely unknown). Next we compare this average ranking with the rankings of the regions that are obtained if we use the  $p_{\text{line}}$  values for each spectral line separately. The quantified difference between the individual and average rankings defines

a “goodness index” for each line. To understand the meaning of this difference we express it in units of the difference that would be expected if the region ranking would be random for a given spectral line. Ideally, for a “perfect” line, the “goodness index” would be zero, while for a bad line (that gives random values) it would be around unity. For 12 of the 20 lines the goodness index is smaller than 0.5. We have selected these 12 lines for use in the inversion while rejecting the other lines. This leaves us with 59 observables and 32 unknowns.

The whole scale of the field strengths  $B_0/k_c^{(2)}$  and  $B_t$  is free floating unless we fix the value of  $B_0/k_c^{(2)}$  for one of the lines before we start the inversion (thus leaving us with 31 unknowns). We have done this for the Ba II 4934 Å line, which has one of the best “goodness” rankings of all our lines, and for which  $B_0$  is found to be 16.3 G from the known life time (obtained from the tables of Wiese & Martin 1980) and Landé factor of its upper state. Since it is a strong line it is formed fairly high in the solar atmosphere, where it can be estimated that the collisional depolarization rate should be negligible in comparison with the natural decay rate, such that  $k_c^{(2)}$  may be assumed to be unity. We thus fix the value of  $B_0/k_c^{(2)}$  for the Ba II 4934 Å line to 16.3 G. As  $k_c^{(2)}$  is always  $\leq 1$ , a value of  $k_c^{(2)}$  that is different from unity would lead to an *increase* of all the derived  $B_t$  values by the factor  $1/k_c^{(2)}$ .

The inversion is done with a standard, non-linear, iterative least-squares fitting technique (cf. Marquardt 1963; Bevington 1969), by minimizing the  $\chi^2$  standard deviation between the model and the data. The problem is thus to find the main minimum of the  $\chi^2$ -hypersurface in the 31-dimensional parameter space. If the problem is ill posed there are many separate hyperspace minima to which the iteration may converge, such that the solution becomes dependent on the starting values that are chosen for the iteration.

The situation is not much helped by finding the global minimum, since there is no assurance why this global minimum should represent the “correct” solution. For any set of minima there will of course always be one that is the deepest, but this by no means implies that it has anything to do with reality. From our experience with inversion techniques, the best way to establish confidence in the validity of a solution is to do many inversion runs with widely separated starting values, both small and large. If all the inversions converge to the same solution, then one may have confidence in it. If there is a dependence on the initial values, then the solution should be discarded.

When running our Hanle inversion problem with the 31 unknowns and 59 observables, we find that all the resulting values of  $B_t$  as well as the values of  $B_0/k_c^{(2)}$  and  $p_0$  for 8 of the 12 spectral lines are independent of all the widely chosen starting values, while the 4 remaining lines are sensitive to the choice of initial values. In spite of the mixed results for the spectral lines the solution for the turbulent field strengths remains stable, which is the main objective of the inversion. Although this stable convergence is no guarantee that our model and reduction procedure are physically correct, it suggests that we are on the right track in our initial attempts to apply the differential Hanle effect for diagnostics of magnetic fields on the solar disk. The

derived values of the turbulent field strengths vary between 4 and 40 G for the 8 solar regions that we have studied.

We here refrain from presenting a tabulation of the numerical values of the solutions for the parameters  $p_0$  and  $B_0/k_c^{(2)}$ , since these values are not at all to be regarded as definite determinations of intrinsic line parameters. They depend on a large number of idealizations, which at the present time were necessary to reach a formal solution. In particular the values depend on our formal and physically questionable procedure of extracting a line polarization, with our crude estimates for the zero point of the polarization scale and the parameter  $\alpha$  in Eq. (8). In future more quantitative work it will be unavoidable to use detailed radiative transfer calculations, since the continuum and line polarizations are so entangled that the formal extraction procedure of Sect. 3.2 in general cannot be trusted. Our main aim with the inversion exercise is rather to illustrate how the differential Hanle effect may in principle be used for diagnostic purposes.

The 20 spectral lines that we started with to explore the differential Hanle effect are all the lines in Figs. 1 and 2 that had an apparently significant polarization signal in solar regions with minimal Hanle depolarization. Most of the lines that did not make it among the final 8 (because they either did not satisfy the “goodness” criterion, or they had unstable convergence) are found in the 5682–5687 Å range of Fig. 2. We do not understand why this is so, but it could be that the application of identical formal extraction procedures for the line polarization to widely separated wavelength regions is incorrect and may lead to internal inconsistencies.

Let us finally note that the line polarizations  $p_{\text{line}}$  and the derived  $p_0$  values are strongly affected by instrumental broadening in the spectrograph and by macroturbulence on the Sun. Our use of the differential polarization effects (line ratios) between different spectral lines and solar regions helps to minimize the possible effects of such broadening on the determined turbulent field strengths.

## 5. Conclusions

Our discovery that spatially varying signatures of Hanle depolarization are common throughout the second solar spectrum has shattered the view that the turbulent magnetic field that fills the space (99 % of the photospheric volume) between the kG flux tubes has unique and invariant properties. The turbulent field strength is not only a function of height in the solar atmosphere — it is a quantity that needs to be mapped and followed in time.

Magnetographs or other Zeeman-effect diagnostics are “blind” to the turbulent fields, since the signals from the many opposite-polarity elements cancel within each spatial resolution element, or within the line-forming region along each line of sight. This is a basic motivation for trying to develop the Hanle effect into a standard diagnostic tool that would allow us to explore magnetoturbulence on the Sun in a parameter domain that is inaccessible by other methods.

The application of Hanle diagnostics on the solar disk is only possible with very sensitive polarimeters, and suitable systems

have not been available in the past. With our ZIMPOL imaging polarimeter we have now reached a sensitivity that makes this domain of physics accessible for exploration and use. Ambiguities in the interpretation can be avoided by doing the observations for combinations of spectral lines with different sensitivities to the Hanle effect. We have shown examples of spectra in which the differential Hanle effect is directly seen. By comparing the appearances of the polarized spectra in different solar regions one can generally conclude by mere visual inspection which solar region has the larger turbulent field strength.

While it is possible to draw such qualitative conclusions from visual inspection without model calculations, we have in the present paper gone a step further and made an attempt to quantify these conclusions, by trying to calibrate the different lines for Hanle diagnostics such that the turbulent field strengths can be determined in units of G. This undertaking has been done in the form of a multi-line, multi-region observational program and an iterative least-squares inversion technique to fit the many free parameters of the problem to the observational constraints. Great care has been taken to condition the problem such that a solution can be obtained that is independent of the initial values used for the iteration. Such a unique convergence could indeed be found for the turbulent field strengths of the 8 solar regions studied, resulting in values ranging from 4 to 40 G for the various regions. These values are consistent with the results of Faurobert-Scholl (1993) and Faurobert-Scholl et al. (1995) from Hanle radiative transfer analysis of the single Sr I 4607 Å line, as well as with the range of field-strength values recently found by Bianda et al. (1997) from observations of Hanle depolarization in the Ca I 4227 Å line.

Our inversion “exercise” has revealed a number of problem areas that urgently need to be dealt with for further progress in this field. One particularly difficult problem is the interaction between the polarizing line and continuum opacities and the question of how to extract from the observed polarization what is due to the line alone, since it is only the line portion that is subject to the Hanle effect. This problem is connected with our inadequate understanding of the continuum polarization, which appears to be substantially larger near the limb than predicted by theoretical models. It is also directly dependent on the accurate positioning of the zero point of the polarization scale, which currently cannot be directly determined from the observations due to Stokes  $I \rightarrow Q$  instrumental cross talk. This effect could be minimized with telescopes that are nearly free from or compensated for instrumental polarization.

For the observational material that we have used for the present inversions we have checked in the 2-D spectral images that there were no significant variations of the polarization along the slit, before the 2-D spectra were contracted to 1-D spectra by spatial averaging. In other ZIMPOL I observations we have examples of spatially varying Hanle depolarization along the spectrograph slit. One such example is illustrated in Fig. 3. It shows how the polarization peak in the Doppler core of the Na I D<sub>2</sub> line exhibits large spatial variations, while the polarization amplitudes in the line wings are practically constant, as expected from the frequency-redistribution theory for the Hanle effect

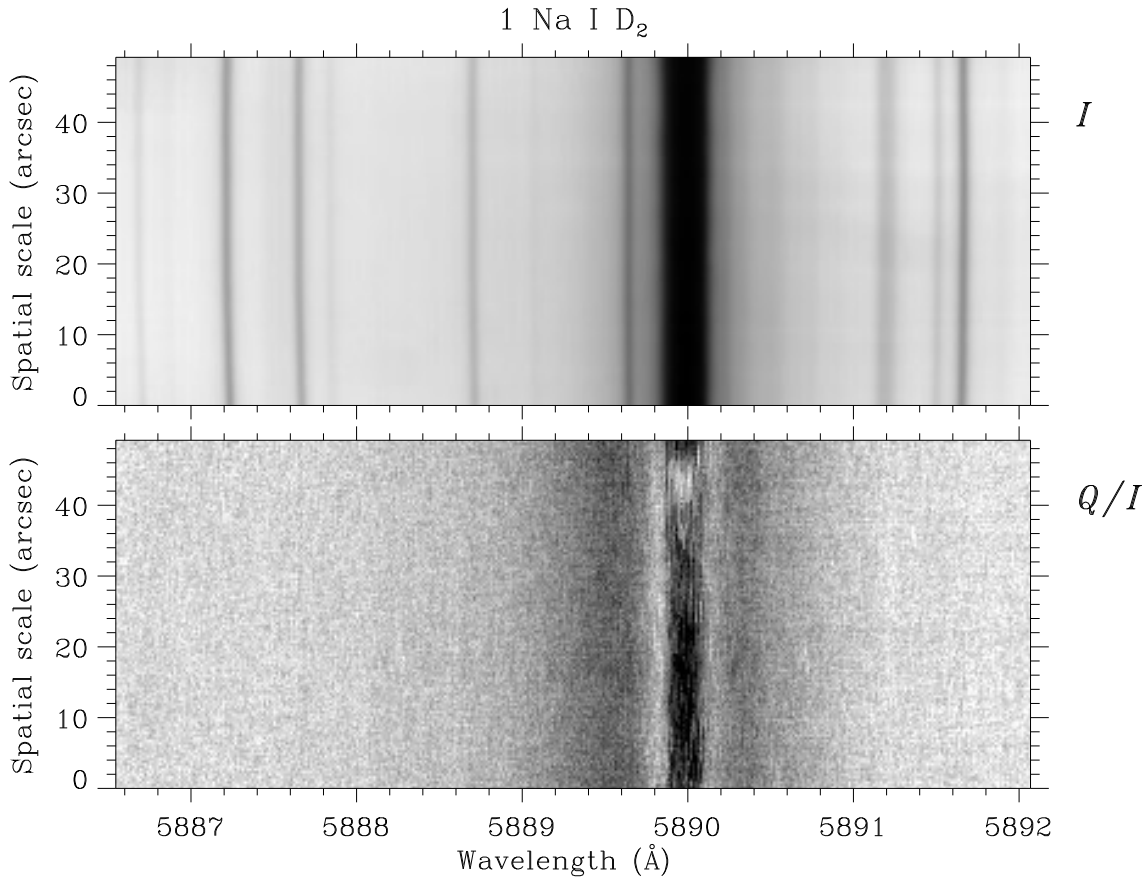


**Fig. 3.** Example of spatially varying Hanle depolarization along the spectrograph slit for the Na I D<sub>2</sub> line. The upper panel shows the intensity  $I$ , while the lower panel shows the fractional linear polarization  $Q/I$ . The slit was parallel to and 5 arcsec inside the solar limb at the position angle corresponding to geographical north. The recording was done with ZIMPOL 1 on 20 February, 1996, at the McMath-Pierce facility of NSO/Kitt Peak. While the polarization amplitude in the line core shows large spatial variations, the polarization maxima in the wings remain relatively constant. This is a characteristic property of the Hanle effect.

(cf. Stenflo 1994). This confirms our interpretation that what we are seeing is really the Hanle effect at work.

The very strong Na I D<sub>2</sub> line is formed substantially higher in the atmosphere than the lines that we have used here for the inversion, so it is likely to be more affected by larger-scale, more ordered magnetic fields in the canopy region of the atmosphere (when observing close to the limb). This also applies to the strong Ca I 4227 Å line in the observations of Bianda et al. (1997), as has been shown by theoretical modelling (Faurobert-Scholl 1992, 1994). The canopy fields are different in nature from the turbulent fields, which are more relevant to the lower parts of the atmosphere. Therefore one has to be careful about the choice of combinations of spectral lines for differential Hanle diagnostics, since the different lines may not sample the same magnetic fields. It could well be that the canopy fields affect to varying degrees also the lines that we have selected here. The height variation of the field needs to be explored in the future. This will require more detailed radiative-transfer modelling of the differential effects in combinations of lines.

The initial magnetic-field models that we have been using are of course by necessity very heuristic and idealized, but as our understanding advances they can be progressively improved upon to higher levels of sophistication, similar to the increased physical realism in the modelling of solar magnetic flux tubes by Zeeman-effect diagnostics. Thus the classification of the magnetic field as being “turbulent”, canopy-like, or in the form of flux tubes is a helpful aid for the present state of the art in Stokes inversion. It allows certain diagnostic regimes to be identified, while the “real” field is more complex. The turbulent fields are expected to occur over a continuous distribution of spatial scales. The microturbulent field that we have addressed here with the Hanle effect may well represent the small-scale end of the spectrum, while the large-scale regime is partly resolved in the form of the intranetwork fields. These intranetwork fields share the properties of flux tubes (by being intermittent) and turbulent fields (by having mixed polarities on small scales), and their field strengths are intermediate between the kG flux tubes in the network and the microturbulent field that is diagnosed with the Hanle effect (Solanki et al. 1996). Eventually the Zee-

man and Hanle diagnostics will be combined in the development of a unified view of solar magnetism.

*Acknowledgements.* We wish to thank the engineering group at ETH Zurich (Peter Povel, Peter Steiner, Urs Egger, Frieder Aebersold), who built the ZIMPOL system and provided the technical support, and Marianne Faurobert-Scholl and Sami Solanki for constructive comments on the manuscript. The ZIMPOL development program and one of us (A.G.) have been funded by the Swiss Nationalfonds, grant no. 2000-043048.95/1. The National Solar Observatory is one of the National Optical Astronomy Observatories, which are operated by the Association of Universities for Research in Astronomy, Inc. (AURA) under cooperative agreement with the National Science Foundation.

## References

- Bianda, M., Solanki, S.K., Stenflo, J.O., 1997, *A&A*, submitted
- Bevington, P.R., 1969, *Data Reduction and Error Analysis for the Physical Sciences*. McGraw-Hill, New York
- Bommier, V., 1980, *A&A* 87, 109
- Faurobert-Scholl, M., 1992, *A&A* 258, 521
- Faurobert-Scholl, M., 1993, *A&A* 268, 765
- Faurobert-Scholl, M., 1994, *A&A* 285, 655
- Faurobert-Scholl, M., Feautrier, N., Machefer, F., Petrovay, K., Spielfeld, A., 1995, *A&A* 298, 289
- Landi Degl'Innocenti, E., 1982, *Solar Phys.* 79, 291
- Leroy, J.-L., Ratier, G., Bommier, V., 1977, *A&A* 54, 811
- Marquardt, D.W., 1963, *J. Soc. Ind. Appl. Math.* 11, 431
- Povel, H.P., 1995, *Optical Engineering* 34, 1870
- Querfeld, C.W., Smartt, R.N., Bommier, V., Landi Degl'Innocenti, E., House, L.L., 1985, *Solar Phys.* 96, 277
- Rüedi, I., Solanki, S.K., Livingston, W., Stenflo, J.O., 1992, *A&A* 263, 323
- Sahal-Bréchet, S., Bommier, V., Leroy, J.-L., 1977, *A&A* 59, 223
- Solanki, S.K., 1993, *Space Sci. Rev.* 63, 1
- Solanki, S.K., Zufferey, D., Lin, H., Rüedi, I., Kuhn, J.R., 1996, *A&A* 310, L33
- Stenflo, J.O., 1973, *Solar Phys.* 32, 41
- Stenflo, J.O., 1982, *Solar Phys.* 80, 209
- Stenflo, J.O., 1987, *Solar Phys.* 114, 1
- Stenflo, J.O., 1994, *Solar Magnetic Fields – Polarized Radiation Diagnostics*. Kluwer, Dordrecht
- Stenflo, J.O., 1997, *A&A* 324, 344
- Stenflo, J.O., Keller, C.U., 1996, *Nature* 382, 588
- Stenflo, J.O., Keller, C.U., 1997, *A&A* 321, 927
- Stenflo, J.O., Baur, T.G., Elmore, D.F., 1980, *A&A* 84, 60
- Stenflo, J.O., Twerenbold, D., Harvey, J.W., 1983a, *A&AS* 52, 161
- Stenflo, J.O., Twerenbold, D., Harvey, J.W., J.W. Brault, 1983b, *A&AS* 54, 505
- Wiese, W.L., Martin, G.A., 1980, *Wavelengths and Transition Probabilities for Atoms and Atomic Ions. Part II. Transition Probabilities*. NSRDS–NBS 68, US Dept. of Commerce